Journal of Archaeological Science: Reports 42 (2022) 103362

Contents lists available at ScienceDirect

Journal of Archaeological Science: Reports

journal homepage: www.elsevier.com/locate/jasrep

Physico-chemical characterisation of remains from a Bronze Age ochre-burial in Biniadris cave (Menorca, Spain)

Pablo Martín-Ramos [a,*], Francisco P.S.C. Gil [b], Jesús Martín-Gil [c]

[a] EPS, Instituto Universitario de Investigación en Ciencias Ambientales (IUCA), University of Zaragoza, Carretera de Cuarte, s/n, 22071 Huesca, Spain
[b] CFisUC, Physics Department, University of Coimbra, Rua Larga, P-3004-516 Coimbra, Portugal
[c] ETSIIAA, Universidad de Valladolid, Avenida de Madrid 44, 34004 Palencia, Spain

ARTICLE INFO

Keywords:
Bone
Biniadris
Bronze Age
Menorca
Pigment

ABSTRACT

Red ochre pigments have been used since ancient times by many different civilisations on different continents. In the paper presented herein, ten manufactured artefacts and biological materials stained with a red pigment found in the Bronze Age burial site of Biniadris Cave (Menorca, Spain) have been characterised throught X-ray fluorescence, X-ray diffraction, Raman and infrared spectroscopy techniques, scanning electron microscopy and energy-dispersive X-ray spectroscopy. The surface analysis of the bones, hairs and ornaments allowed the chemical composition of the pigment used in the funeral practices and rituals to be unequivocally established as hematite-rich ochre. The finding of a gypsum preparation layer on a sample, below the ochre layer, suggests that it could have been used as a primer before sprinkling with hematite ochre. Given the excellent degree of conservation and the worth of this archaeological record for the study of the symbolic practices in the island of Menorca, these results call for further analyses on a larger set of archaeological artefacts to gain insight into the funeral practices conducted in this cave.

1. Introduction

The use of red pigment of mineral origin, commonly ochre, has been a constant feature of prehistoric mankind since the Middle Stone Age in Africa when engraved stones from the Blombos site were daubed with haematite (Watts, 2009). In Europe, there is also evidence that Neanderthals felt a similar fascination for the red colour (Roebroeks, et al., 2012), but it was not until the Upper Palaeolithic when ochre became the pigment par excellence in cave paintings (Marshack, 1981) and, above all, when its presence became widespread in burials. The famous Red Lady of Paviland, or the more recently discovered Red Lady of El Mirón, are only the tip of the iceberg of a far-reaching phenomenon −that of ochre-dusted tombs from the end of the Palaeolithic (Gambier, 2008, Giacobini, 2006)−, which includes dozens of emblematic burials such as the triple inhumation at Barma Grande de Grimaldi, the mythical Cromagnon burial discovered by Lartet, the infant burial at Lagar Velho in Portugal, or some of the Pavlovian tombs from Dolni Vestonice (Grünberg, 2012, Neugebauer-Maresch, 2012, Pettitt, 2011).

Rather than practical, the use of red pigments in tombs may have had symbolic purposes: in the case of ochre from Palaeolithic tombs, apart from the mere aesthetic consideration, a ritual intention is usually presumed (red as a symbolic colour for blood, life or menstruation), not incompatible with a certain utilitarian character of haematite, as a neutraliser of bad smells or as a tanning agent (Cortell Nicolau, 2016). The same applies to Mesolithic sites (Grünberg, 2012), such as the Iberian burials at Los Canes, in Asturias (Arias and Garralda, 1996); Mas Nou, in Castellón (Olaria Puyoles, 2002); or La Braña-Arintero cave, in León (Vidal Encinas, et al., 2008).

The presence of red pigments in burials persisted over time. In Iberia, from the early 4th millennium BC it has been documented in a number of Late Neolithic and Copper Age collective tombs. The most eloquent testimonies are reported in Extremadura, Andalusia and southern Portugal. With regard to the Balearic Islands, reports on the use of red pigments are limited to two Menorcan caves: *Rubia* spp. extracts were used for hair dying in the Es Càrritx Cave (Lull, et al., 1999), and the presence of a mineral pigment −presumably ochre− was referred by Alarcón García, et al. (2016) in Biniadris Cave.

Biniadris Cave is an 18 m^2 natural cavity located on a cliff face in the southeast of the island of Menorca (Spain), excavated in a dolomitised biocalcarenite (rudstone), typical of the Menorcan coastline, where the lithology of calcarenites and calcisiltites is omnipresent (Fornós, 2003). Discovered in 2009 by the UEM speleology group and first studied in

* Corresponding author.
E-mail address: pmr@unizar.es (P. Martín-Ramos).

https://doi.org/10.1016/j.jasrep.2022.103362
Received 15 November 2020; Received in revised form 23 July 2021; Accepted 20 January 2022

2013, Biniadris Cave is part of the Cales Coves necropolis and is similar to other funeral caves found in the area since 1990, such as Es Mussol, Es Càrritx and Es Pas, except for its exceptional degree of conservation (Moreno Onorato, et al., 2019). It was inhabited around 3,400 years ago (Naviform Period, 1740–1400 BCE) and, according to the preliminary archaeological results, the cave would not have been just an ossuary, but a sacralised space in which the practices of burial, together with the trousseaux that accompanied the corpses, acquired a predominant symbolic role (Alarcón García, et al., 2016).

Skulls, ribs and other human bones from almost 100 individuals of different ages and an assortment of clothing and personal objects were buried inside (Altamirano García and Alarcón García, 2018). Among these remains, a set of 14 buttons with V-perforation came to light −out of which 11 were made from bone and the other 3 from wild boar tusk−, 2 pointed elements, 3 circular pieces of bone decorated with concentric rings and a possible pendant on a swine tusk. These accessories were deposited with the deceased during the funeral rituals. Moreover, a red pigment was observed covering remains of human hair and most of the surface of six of the buttons as an additional decorative element.

In the case of bone buttons with V-shaped perforation −a recurrent element in archaeological sites from the third millennium B.C., coinciding in time with the Bell Beaker culture−, it has been indicated (Alarcón García, et al., 2016) that in most cases they are segments obtained from the diaphysis of long bones (metapodials or tibiae) from large animals (deer, bovine) and, in three cases, from tusks of members of the Suidae family (pig or wild boar). The worn-out surface of the buttons would be consistent with prolonged use over time, suggesting that they could have been inherited from generation to generation (Altamirano García, 2014). With regard to the impregnation of six of the buttons with a red mineral, possibly 'ochre' (Altamirano García and Alarcón García, 2018), it has been linked to a type of ritual previously identified in Es Càrritx, in which the hair of the deceased was dyed with madder red and then cut and stored in small containers with worked bone covers (Alarcón García, et al., 2016).

Taking into consideration that pigment use in the Bronze Age in Europe is poorly documented, that the context of burials may allow addressing pigment use as part of complex symbolic practices, and that the presence of red coatings on hairs and buttons is not a usual discovery in prehistoric and proto-historic times in Europe, physico-chemical characterisation of some the archaeological materials recovered from Biniadris Cave in 2015 and 2017 archaeological campaigns was required. Hence, in this work, X-ray fluorescence (XRF), X-ray powder diffraction (XRPD), Raman and infrared spectroscopy techniques, scanning electron microscopy (SEM) and energy-dispersive X-ray spectroscopy (EDX) analytical techniques have been applied to identify the aforementioned red pigment.

2. Materials and methods

2.1. Samples

Among the materials recovered from the cave in the 2015 and 2017 excavation campaigns, several manufactured artefacts and biological objects/materials (bones, hairs), along with a mineral pigment, were studied. A subadult rib with red pigment (*#11671*, Fig. 1); a fragment of skull stained with red pigment (*#1132-14*, Fig. 2a); a non-defined piece of human bone (*#1584-10*); and two samples of human hair presumably impregnated with red pigment (*#12493-15* and *#12032-10*) were analysed. The animal bone samples were four V-perforated buttons with red pigment impregnation (*#1903, #1904, #1905*, and *#1879-6*; see Fig. 2b-d), and finally a mineral sample with red-ochre aspect (*#12969*).

2.2. Characterisation

X-ray fluorescence spectroscopy was used to determine the elemental composition of the materials, by means of a Niton XL3t GOLDD+ portable analyzer (Thermo Fisher Scientific, Waltham, MA, USA). X-ray tube: Au anode, 50 kV, 200 μA; spot size: 8 mm; 3 mm small-spot collimation. TestAll™ Geo mode was used, with at least 3 measurements per analysis, with a 240 s acquisition time/measurement.

Fig. 1. Photograph of a subadult rib with red pigment (*#11671*). (For interpretation of the references to colour in this figure legend, the reader is referred to the web version of this article.)

The powder diffractograms of the samples were acquired using a D8 Advance Bragg-Brentano diffractometer (Bruker, Billerica, MA, USA), with a CuKα ($\lambda = 1.54$ Å) radiation source, in reflection mode. Crystalline silicon was used as a standard. Experimental conditions: 40 kV, 40 mA; $2\theta = 5 - 80^\circ$, step: 0.02°, 1 s/step. DIFFRAC.EVA software was used for phase analysis. Up-to-date International Centre for Diffraction Data (ICDD) and Crystallography Open Database (COD) databases were used for peak identification.

Raman spectra were obtained with a Jobin–Yvon T64000 apparatus (Horiba Scientific, Kyoto, Japan). Spectra were acquired in the 4000–50 cm^{-1} range at 3 cm^{-1} spectral resolution on a micro-Raman spectroscope with a Nd:YAG laser excitation source (1064 nm line, 100 mW). Experimental conditions: 0.64 m focal length, f/7.5 aperture, 1800 gr/mm diffraction gratings, single-channel detection (with a R943 photomultiplier), and a 1024 × 256 px nitrogen-cooled 1″ CCD detector. A minimum of three spectra were collected per analysis.

A Nicolet iS50 Fourier-Transform Infrared (FTIR) spectrometer (Thermo Fisher Scientific) with a built-in attenuated total reflection (ATR) module was used for infrared spectra characterisation. ATR-FTIR spectra were collected in the 400–4000 cm^{-1} range at 1 cm^{-1} spectral resolution, co-adding 128 scans. The advanced ATR correction algorithm available in OMNIC™ software suite (Nunn and Nishikida, 2008) was used to correct band intensity distortion, peak shifts and non-polarisation effects created by the ATR technique.

SEM and EDX analyses were conducted with an EVO HD 25 (Carl Zeiss, Oberkochen, Germany) apparatus. Experimental conditions: electron high tension (EHT) = 15 kV, probe current = 4–12 pA; working distance (WD) = 8.5–10.5 mm.

3. Results

3.1. Elemental analyses by X-ray fluorescence spectroscopy

Major (Ca, S and P) and minor (Zn, Fe, K, Al, Si and Cl) elements found in the ten samples from Biniadris funeral cave are summarised in Table 1. Trace elements can be found in Table S1.

Ca and P are related and their high concentrations in all bone samples were consistent with the expected composition (i.e., hydroxyapatite and apatite carbonate). The presence of Al, Si, K and Cl would have an edaphological origin.

Human remains, depending on whether they were bones or hair, had different contents not only in S, K, Al and Cl main elements, but also in trace elements such as As, Zn, W, Cu, Mn, Sc, Cs, Rb, Sb, Te, Sn, Cd and Pd.

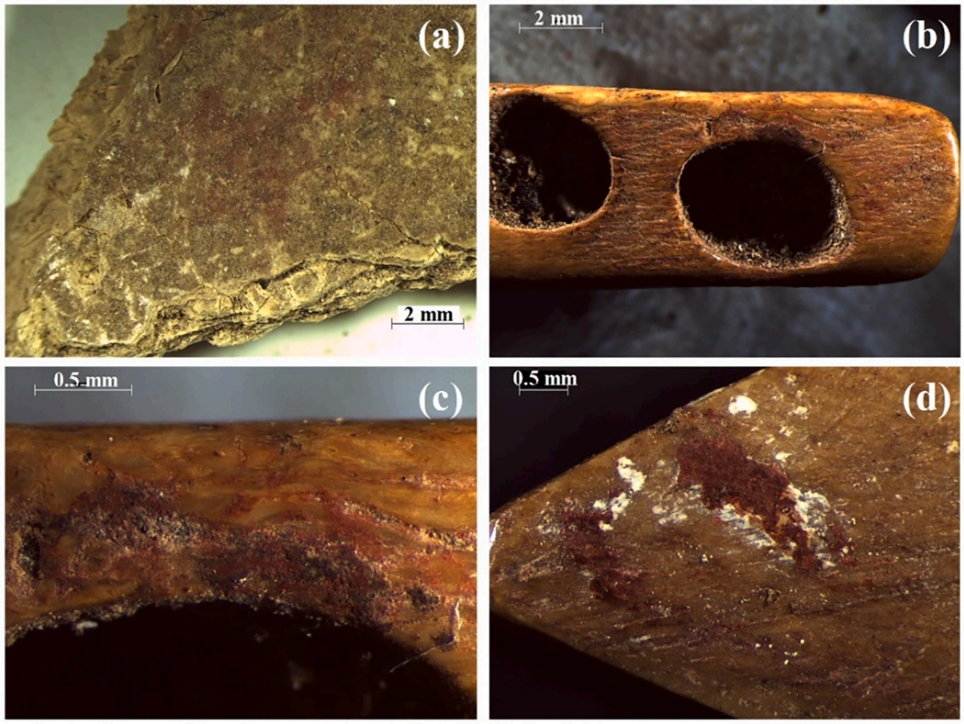

Fig. 2. Micrographs of (*a*) a human skull (*#1132-14*) and V-perforated button samples ((*b-c*) *#1903-003*, (*d*) *#1904*) impregnated with red-ochre pigment. Credit: Dr. E. Alarcón-García (Departamento de Prehistoria y Arqueología, Universidad de Granada, Spain). (For interpretation of the references to colour in this figure legend, the reader is referred to the web version of this article.)

Table 1
Elemental analysis of the Biniadris funeral cave samples by XRF. Results are expressed as wt% and as wt%/(Ca + P), respectively. Values are reported as an average of three measurements.

Sample	Zn	Fe	Ca	K	S	Al	P	Si	Cl
Human rib (*#11671*)	-/-	8.0/38	70.5/-	0.7/3.5	6.2/29.7	-/-	8.4/-	3.4/16.3	2.1/9.8
H. bone (*#1584-10*)	-/-	3.0/23.5	61.0/-	0.4/3.2	2.5/19.4	1.8/13.8	26.2/-	3.7/29.0	0.9/7.2
Skull (*#1132-14*)	-/-	0.6/3.6	62.5/-	1.2/6.8	5.0/28.5	2.4/3.8	19.8/-	5.7/32.0	2.4/13.7
Hair (*#12032-10*)	-/-	8.3/-	26.8/-	2.2/	30.1/-	-/-	-/-	13.1/-	7.0/-
Hair (*12493-15*)	-/-	4.4/-	44.4/-	2.3/	30.0/-	-/-	3.0/	4.2/-	8.7/-
V-button (*#1904*)	-/-	1/6.5	62.2/-	0.4/2.7	8.5/57.8	0.6/4.8	23.1/-	1.9/12.8	2.1/14.0
V-button (*#1903*)	-/-	0.2/2.0	61.5/-	0.5/3.9	6.1/52.7	0.6/5.6	26.9/-	1.6/13.5	2.3/20.3
V-button (*1905*)	-/-	0.2/1.6	62.0/-	0.4/2.7	9.3/68.7	-/-	24.4/-	1.3/9.8	2.0/14.8
V-button (*#1879-6*)	0.1/1.9	0.2/4.3	63.9/-	0.3/5.4	2.0/36.3	-/-	30.7/-	1.0/18.5	1.7/31.0
Mineral (*#12969*)	-/-	2.5/-	51.4/-	-/-	-/-	8.1/	-/-	8.8/-	1.0/-

V-buttons made from animal bones showed significantly lower contents in Fe, Al and Si –and in As, Cu, Ni and Sn trace elements– than human bones.

The mineral sample with ochre aspect, *#12969*, showed high contents of Si, Al and Mg, and of minor and trace elements (Cu, Cr, Th, V and Sc).

3.2. X-ray powder diffraction analyses

The XRPD patterns from two samples are shown in Fig. 3. The diffractogram of the red-stained bone (*#1584–10*) mainly corresponded to carbonate-hydroxyapatite, with weaker peaks compatible with the presence of hematite (at $2\theta = 33.19^\circ$, 35.67°, 49.52°, 54.13° and 64.08°), while the main diffraction peaks in the presumable ochre mineral sample (*#12969*) could be attributed to gypsum (COD 2300258). The strong peak at $2\theta = 26.15^\circ$, not attributable to gypsum, may be associated with presumable graphite impurities (COD 9012705) in carbonaceous materials (such as carbon black or coal).

3.3. Raman vibrational analyses

The Raman spectra of the surface of a V-perforated button and the subadult rib with red pigment are shown in Fig. 4. The peaks in the spectrum of the white area (Fig. 4a) were associated with gypsum, while those present in the spectra collected from red areas (Fig. 4b-c) showed a good correspondence with iron compounds. Specifically, the peaks at 216–222, ~280 and 597–613 cm^{-1} are attributable to hematite (Fe-O bending in the former, and the Fe-O stretching in the latter two); that of 1011 cm^{-1} to gypsum, anhydrite or natrojarosite (S-O str.); that of 1123 cm^{-1} to gypsum or anhydrite (S-O str.) (Ambers, 2004); and those of 1280 cm^{-1} and 1582 cm^{-1} to D and G-modes of carbonaceous materials, respectively (Legodi, 2008, Xie et al., 2019).

Among the iron oxides and hydroxides that can feature stronger Raman scattering, such as hematite (α-Fe_2O_3), goethite (α-FeOOH), lepidocrocite (γ-FeOOH), and akaganeite (β-FeOOH), the former is the most frequently found either in case of corrosion at high temperature and for buried artefacts (Bellot-Gurlet, et al., 2009).

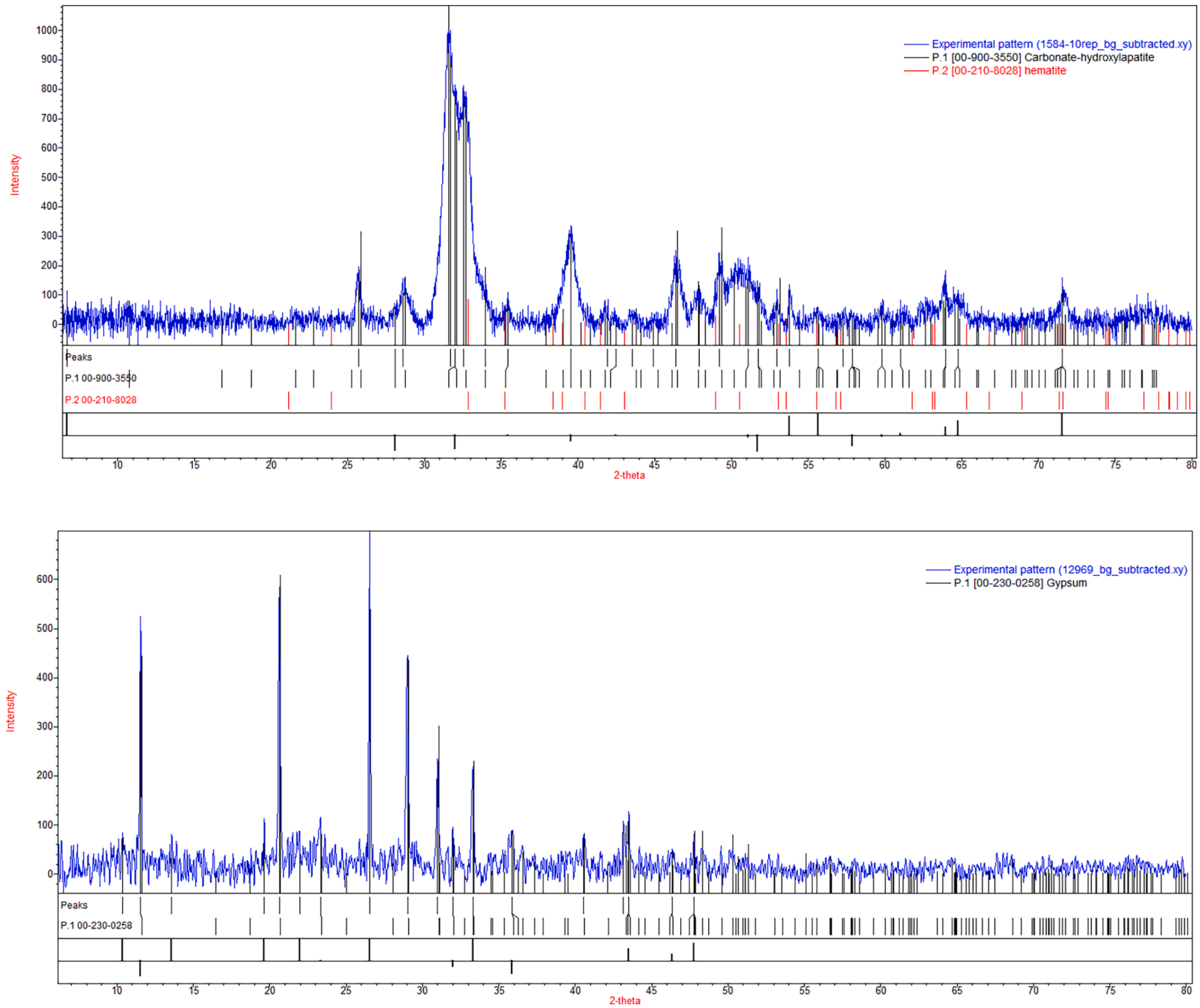

Fig. 3. Powder diffractograms of: (*top*) a subadult rib sample (*#1584-10*); and (*bottom*) a red-ochre mineral sample (*#12969*). (For interpretation of the references to colour in this figure legend, the reader is referred to the web version of this article.)

3.4. *FTIR analyses*

An analysis of the FTIR spectrum (Fig. 5) of the red pigment that covered the subadult rib (*#11671*) allowed to observe not only the presence of hematite (LO and TO phonon modes at 669 and 526 cm^{-1}, respectively) and maghemite (LO and TO phonon modes at 457 and 444 cm^{-1}, respectively) (Jubb and Allen, 2010), but also that of well-preserved bone type I collagen (amide I, β-sheets at 1622 cm^{-1}, amide II at 1558 cm^{-1}, and carboxyl group –wagging vibration of proline side chains– at 1339 cm^{-1}) (Chadefaux, et al., 2009, Wang, et al., 2006). Additional bands could be assigned to carbonate apatite (1418 cm^{-1}, COO^- str./CO_3^{2-} B str.; and 873 cm^{-1}, CO_3^{2-} out-of-plane bending) (Antonakos, et al., 2007) and phosphate (1027 cm^{-1} asymmetric P–O stretching vibrations from hydroxyapatite and 1110 cm^{-1} due to the presence of mineral phase brushite, HPO_4^{2}, which occurs in bone fractures) (Jastrzębski, et al., 2011, Spevak, et al., 2013, Vallejo-Valdezate, et al., 2000).

3.5. *SEM-EDX study*

Although the optical microscopy images (Fig. 2) allowed us to observe the location and even the density of the Fe-based pigment, both the content in this element and its distribution were confirmed by EDX analyses and by comparison of SEM micrographs with elemental mappings. Fig. 6 and Fig. 7 show the SEM base images and the elemental mapping for Ca and Fe of the red accretions on samples *#1904* and *#11671*. The content of Fe and the distribution densities were higher for the V-button sample (*#1904*) than for the human rib sample (*#11671*).

4. Discussion

It should be clarified that –as regards the study of the pigment composition– the sensitivity to the surface composition of both XRF and XRPD techniques would be limited by the fact that X-rays penetrate deeply in the bulk medium and the pigment layers under study were very shallow. Furthermore, in the case of XRPD, the inability to finely grind the archaeological samples to fine powder would prevent the creation of a flat upper surface. Thus, the results from these two techniques should be taken with caution. On the other hand, Raman spectroscopy results may be regarded as the most reliable, provided that this technique is particularly well suited to provide either functional group or structural information about a surface (Tian and Ren, 2006). These vibrational spectroscopy results were conclusive about the presence of hematite.

Intentional uses of hematite-rich red ochres as pigments, partly due to their good preservation, are global. Evidence of their widespread use

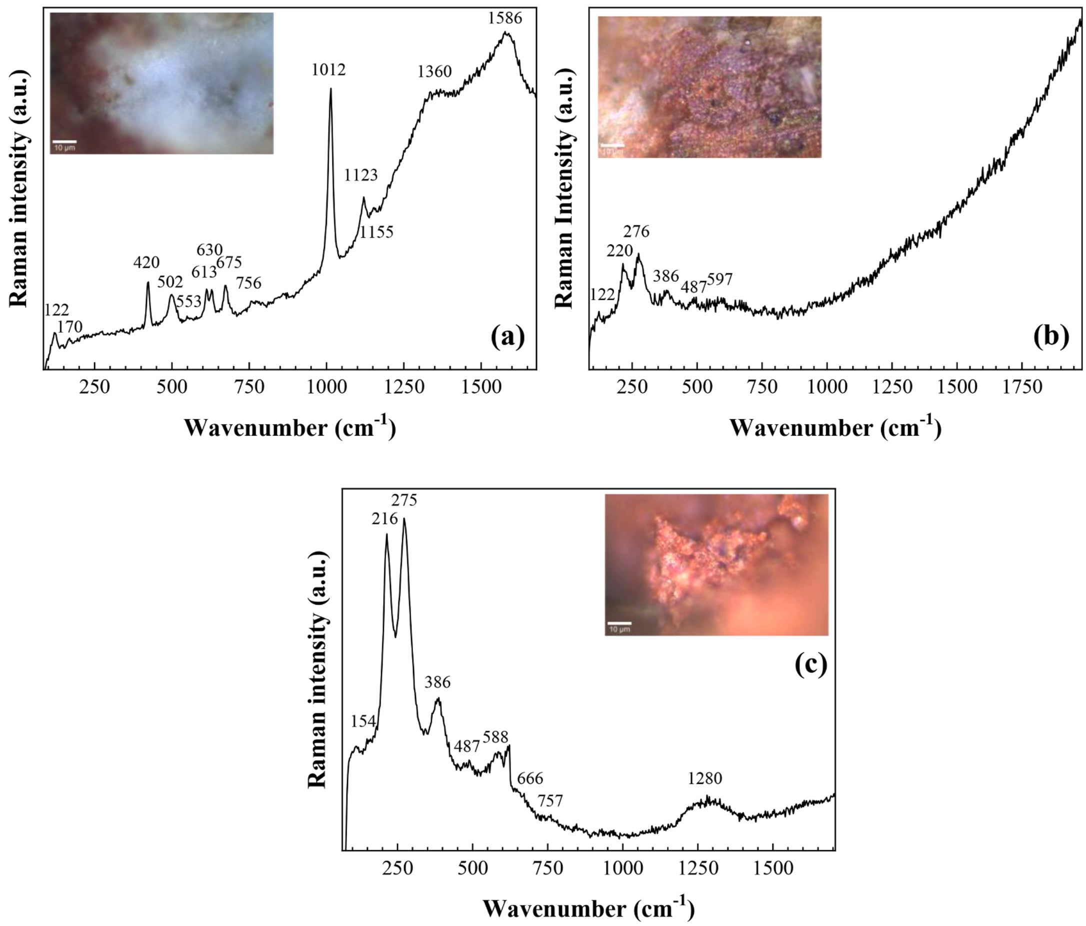

Fig. 4. Raman spectra of: (*a*) white region and (*b*) red region on the surface of the V-perforated button (*#1904*); and (*c*) red region on the surface of the subadult rib sample (*#11671*). (For interpretation of the references to colour in this figure legend, the reader is referred to the web version of this article.)

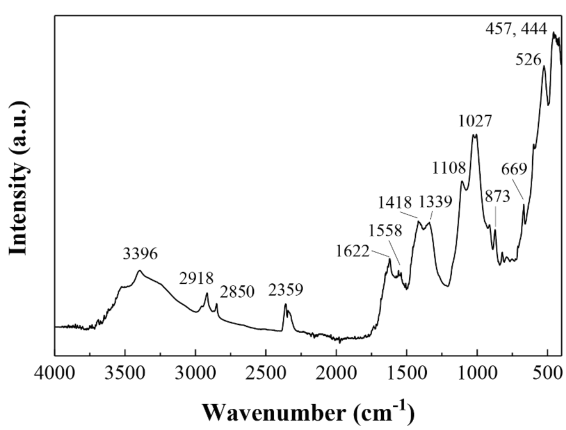

Fig. 5. Infrared spectra of the red region on the surface of the subadult rib sample (*#11671*).

may be found in works of art from all periods. The processing of iron oxide ores to obtain pigments is simple and involves an operational sequence (*chaîne opératoire*) that consists in an initial removal of larger impurities (e.g., plant roots) followed by comminution (viz., grinding, sieving and/or elutriation (levigation)) and final dispersion in a medium to yield a paint.

The red pigment found in the manufactured artefacts and biological materials was allochthonous (the nearest iron mineral deposits would be those reported in Ferrerías, *ca.* 25 km from the site) and, given the parallels of the ritual process conducted in the cave with those reported in other burial caves spread throughout the island (Moreno Onorato, et al., 2019), the staining was clearly intentional (i.e., it did not come from the environment sediment or as a secondary phase formed at the surface of the bone after burying).

As regards ochre (hematite) distribution, some human remains (in particular a rib and a hair sample) were the most covered with hematite, suggesting direct and deliberate staining using this mineral. Animal bone artefacts also showed ochre coating. Even though the covering of human bodies with ochre was a frequent practice in Europe since Upper Paleolithic, covering with red ochre animal bones or animal bone artefacts is not common (Larsson, 1989, Liesau, et al., 2013), which can be regarded as a peculiar feature of the findings reported herein.

The finding of well-preserved bone type I collagen in the red pigment that covered the subadult rib (*#11671*) would support the hypothesis of Keeley (1980), who suggested that red ochre inhibits collagenase and would be used for preserving purposes (e.g., to 'tan' animal hides).

The use of hematite ochres in combination with other minerals is a matter of major discussion. As noted by Henshilwood, et al. (2011), the combination and usage of substances as pigments can be regarded as a reference point in terms of the evolution of complex human cognition. In Biniadris Cave, human hair and bones appeared covered by hematite, but –as noted above– some samples (*#1904*) also contained gypsum (evident in Fig. 6a), which was the main constituent of the mineral fragment (*#12969*). Although it cannot be ruled out that gypsum could have been used as an extender to bulk out the pigment, its presence below the red ochre layer suggests that it would probably have been used as a ground for painting (i.e., as a primer on some bones before they were sprinkled with hematite ochre) (Siddall, 2018).

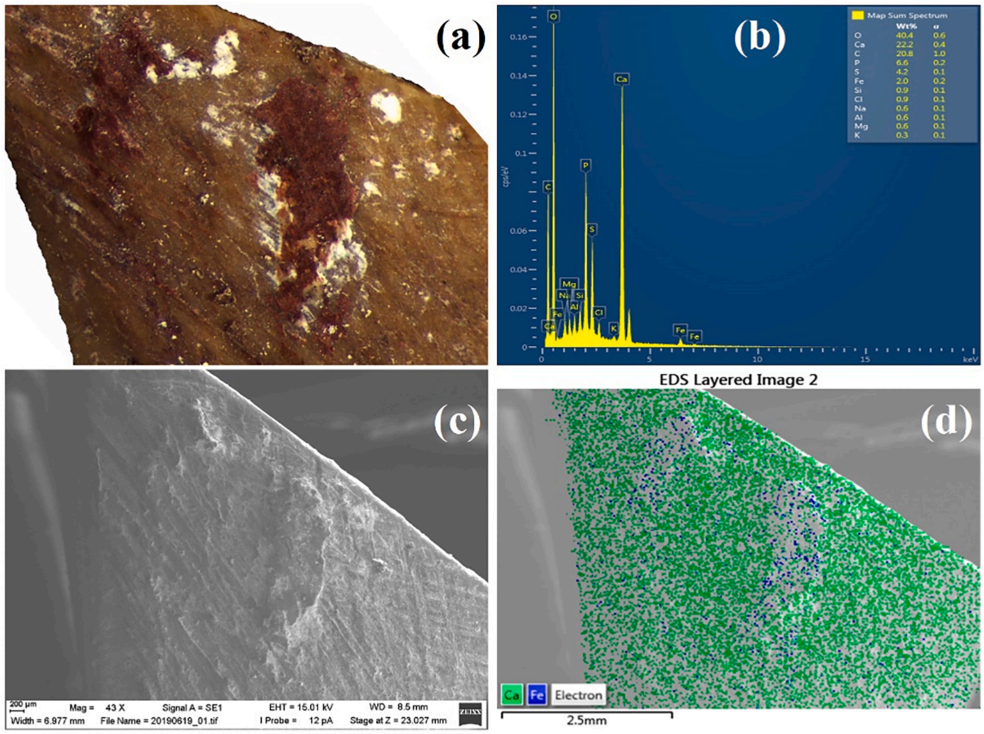

Fig. 6. (*a*) Optical micrograph, (*b*) EXD spectrum, (*c*) SEM base image, and (*d*) elemental mapping for Ca and Fe content of the surface of V-button *#1904*.

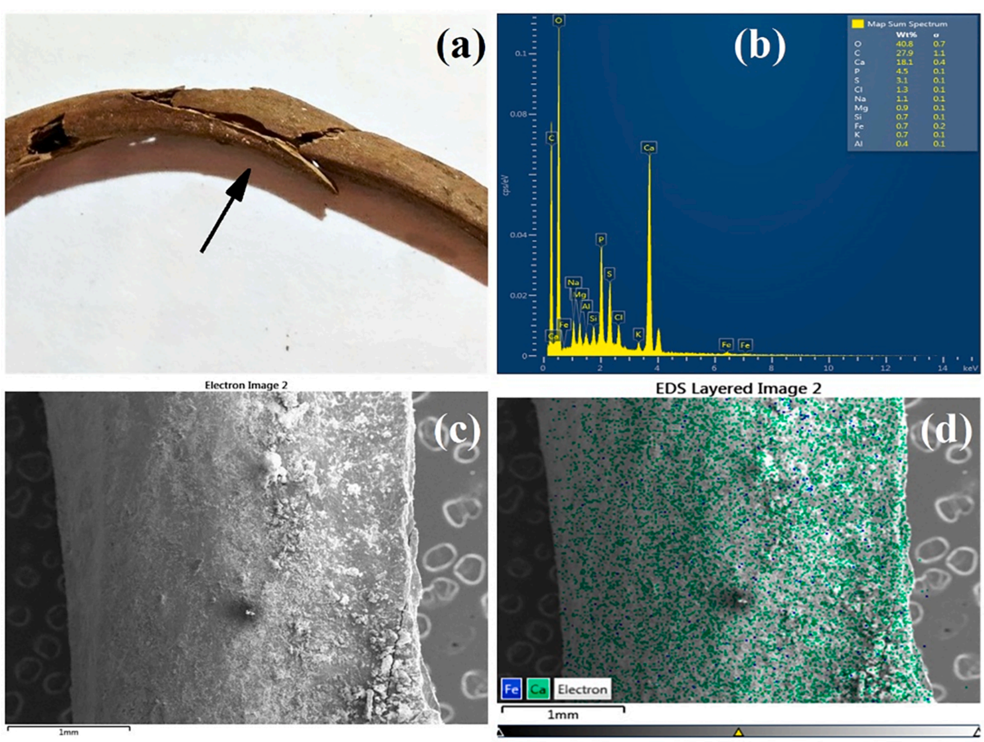

Fig. 7. (a) Photograph showing the sampled area, (b) EDX spectrum, (c) SEM base image and (d) SEM map image showing Ca and Fe distribution on a zone of the subadult rib sample (*#11671*).

5. Conclusions

Analytical data obtained from a variety of techniques (XRF, XRPD, Raman and FTIR spectroscopies and SEM-EDX) on a set of archaeological remains objects retrieved from Biniadris Cave (Menorca, Spain) confirmed the use of hematite-rich red ochre on bones, hair and artefacts in burial rituals around 3400 years ago. The presence of a gypsum coating on an ornament (a button) below the ochre layer suggests that it may have been used as a primer before it was sprinkled with hematite ochre, thus pointing to sophisticated knowledge of the use of this pigment. Future studies are needed to deepen our understanding of Bronze Age ochre-centred funeral rituals on the island of Menorca.

CRediT authorship contribution statement

Pablo Martín-Ramos: Methodology, Formal analysis, Investigation, Writing-original draft, Writing-review & editing, Visualisation. **Francisco P.S.C. Gil:** Formal analysis, Investigation, Validation, Writing-original draft. **Jesús Martín-Gil:** Conceptualisation, Formal analysis, Investigation, Resources, Writing-original draft, Funding acquisition.

Declaration of Competing Interest

The authors declare that they have no known competing financial interests or personal relationships that could have appeared to influence the work reported in this paper.

Acknowledgements

The authors gratefully acknowledge Dr. Eva Alarcón-García (Department of Prehistory and Archaeology, University of Granada) and the Consell Insular de Menorca for kindly facilitating access to the archaeological remains under study. Access to TAIL-UC facility funded under QREN-Mais Centro project ICT-2009-02-012-1980 and to the GeoSciences Centre of Department of Earth Sciences XRF equipment at FCTUC (Prof. Lídia M. Gil Catarino) is also acknowledged.

Appendix A. Supplementary data

Supplementary data to this article can be found online at https://doi.org/10.1016/j.jasrep.2022.103362.

References

Alarcón García, E., Moreno Onorato, A., Arboledas Martínez, L., Mora González, A., Díaz-Zorita, M., Orfila Pons, M., 2016. Cueva de Biniedrís: una historia por contar. Revista de Menorca 95, 156–184.

Altamirano García, M., 2014. Uso y mantenimiento de objetos, botones y peines de márfil, huesos y asta de ciervo de Los Castillejos de Montefrío (Granada). Antiquitas 155–160.

Altamirano García, M., Alarcón García, E., 2018. Bone tools for the deceased: approaches to the worked osseous assemblage from the Bronze Age funerary cave of Biniadris (Menorca, Spain). Quat. Int. 472, 108–114.

Ambers, J., 2004. Raman analysis of pigments from the Egyptian Old Kingdom. J. Raman Spectrosc. 35 (89), 768–773.

Antonakos, A., Liarokapis, E., Leventouri, T., 2007. Micro-Raman and FTIR studies of synthetic and natural apatites. Biomaterials 28 (19), 3043–3054.

Arias, P., Garralda, M.D., 1996. Mesolithic burials in los canes cave (Asturias, Spain). Human Evolution 11 (2), 129–138.

Bellot-Gurlet, L., Neff, D., Réguer, S., Monnier, J., Saheb, M., Dillmann, P., 2009. Raman studies of corrosion layers formed on archaeological irons in various media. J. Nano Res. 8, 147–156.

Chadefaux, C., Le Hô, A.-S., Bellot-Gurlet, L., Reiche, I., 2009. Curve-fitting Micro-ATR-FTIR studies of the amide I and II bands of type I collagen in archaeological bone materials. E-Preservation Science 6, 129–137.

Cortell Nicolau, A., 2016. El ocre en la Prehistoria: entre la funcionalidad y el simbolismo. Archivo de prehistoria levantina 187–211.

Fornós, J.J., 2003. El karst y la evolución del litoral del Migjorn de Menorca, Introducción a la Geografía Física de Menorca. Mon. Soc. Hist. Nat. Balears 10, 101–110.

Gambier, D., 2008. Les sujets juvéniles du Paléolithique supérieur d'Europe à travers l'analyse des sépultures primaires : L'exemple de la culture gravettienne, in: Gusi, F., Olaria, D.C., Muriel, L.S. (Eds.), La muerte en la infancia, Servicio de Investigaciones Arqueologicas y Prehistoricas de la Diputación de Castellón, Castellón, Spain, pp. 331-364.

Giacobini, G., 2006. Richesse et diversité du rituel funéraire au paléolithique supérieur. Diogène 24–46.

Grünberg, J., 2013. Rot in paläolithischen und mesolithischen Bestattungen, in: Meller, H., Wunderlich, C.H., Knoll, F. (Eds.), Rot – Die Archäologie bekennt Farbe. 5. Mitteldeutscher Archäologentag vom 4. bis 6. Oktober 2012 in Halle (Saale), Tagungen des Landesmuseums für Vorgeschichte Halle, Halle, pp. 121-134.

Henshilwood, C.S., d'Errico, F., van Niekerk, K.L., Coquinot, Y., Jacobs, Z., Lauritzen, S.-E., Menu, M., García-Moreno, R., 2011. A 100,000-Year-Old Ochre-Processing Workshop at Blombos Cave, South Africa. Science 334 (6053), 219–222.

Jastrzębski, W., Sitarz, M., Rokita, M., Bułat, K., 2011. Infrared spectroscopy of different phosphates structures. Spectrochim. Acta Part A Mol. Biomol. Spectrosc. 79 (4), 722–727.

Jubb, A.M., Allen, H.C., 2010. Vibrational Spectroscopic Characterization of Hematite, Maghemite, and Magnetite Thin Films Produced by Vapor Deposition. ACS Appl. Mater. Interfaces 2 (10), 2804–2812.

Keeley, L.H., 1980. Experimental Determination of Stone Tool Uses: A Microwear analysis. University of Chicago Press, Chicago.

Larsson, L., 1989. Big dog and poor man. Mortuary practices in Mesolithic Societies in Southern Sweden, in: Larsson, T.B., Lundmark, H. (Eds.), Approaches to Swedish Prehistory. A spectrum of problems and perspectives in contemporary research, B.A. R., Oxford, pp. 211-223.

Legodi, M.A., 2008. Raman spectroscopy applied to iron oxide pigments from waste materials and earthenware archaeological objects, Chemistry, University of Pretoria, Pretoria, South Africa, p. 106.

Liesau, C., Daza, A., Llorente, L., Morales, A., 2013. More questions than answers: the singular animal deposits from Camino de Las Yeseras (Chalcolithic, Madrid, Spain). Anthropozoologica 48 (2), 277–286.

Lull, V., Micó, R., Rihuete, C., Risch, R., 1999. La Cova des Càrritx y la Cova des Mussol. Ideología y sociedad en la prehistoria de Menorca, Consell Insular de Menorca, Mahon.

Marshack, A., 1981. On Paleolithic ochre and the early uses of color and symbol. Curr. Anthropol. 22 (2), 188–191.

Moreno Onorato, A., Alarcón García, E., Díaz-Zorita Bonilla, M., Arboledas Martínez, L., 2019. El descubrimiento de la cueva de Biniedrís (Alaior, Menorca, España). Revista de Menorca 98, 271–286.

Neugebauer-Maresch, C., Hammer, V., Einwögerer, T., Händel, M., Simon, U., 2013. Die gravettienzeitlichen Rötelgräber und die Farbstoffe des Fundplatzes Krems Wachtberg/Niederösterreich, in: Meller, H., Wunderlich, C.H., Knoll, F. (Eds.), Rot – Die Archäologie bekennt Farbe. 5. Mitteldeutscher Archäologentag vom 4. bis 6. Oktober 2012 in Halle (Saale), Tagungen des Landesmuseums für Vorgeschichte Halle, Halle, pp. 135-141.

Nunn, S., Nishikida, K., 2008. Advanced ATR Correction Algorithm - Application Note 50581. ThermoScientific, Madison, WI, USA.

Olaria Puyoles, C.R., 2002. La muerte como rito tanscendental: los rituales funerarios del epipaleolítico-mesolítico y su probable influencia en el mundo megalítico. Quaderns de prehistòria i arqueologia de Castelló 85–106.

Pettitt, P., 2011. The Palaeolithic origins of human burial, Routledge, Milton Park, Abingdon, Oxon ; New York.

Roebroeks, W., Sier, M.J., Nielsen, T.K., De Loecker, D., Pares, J.M., Arps, C.E.S., Mucher, H.J., 2012. Use of red ochre by early Neandertals. Proc. Natl. Acad. Sci. 109 (6), 1889–1894.

Siddall, R., 2018. Mineral pigments in Archaeology: Their analysis and the range of available materials. Minerals 8 (5), 211. https://doi.org/10.3390/min8050201.

Spevak, L., Flach, C.R., Hunter, T., Mendelsohn, R., Boskey, A., 2013. Fourier transform infrared spectroscopic imaging parameters describing acid phosphate substitution in biologic hydroxyapatite. Calcif. Tissue Int. 92 (5), 418–428.

Tian, Z.-Q., Ren, B., 2006. Infrared and Raman spectroscopy in analysis of surfaces. In: Meyers, R.A., McGuire, G.E. (Eds.), Encyclopedia of Analytical Chemistry. John Wiley & Sons Ltd., pp. 1–40

Vallejo-Valdezate, L.A., Martin-Gil, J., Jose-Yacaman, M., Martin-Gil, F.J., Gil-Carcedo, L.M., 2000. Scanning electron microscopy images and energy-dispersive X-ray microanalysis of the stapes in otosclerosis and Van der Hoeve syndrome. Laryngoscope 110, 1505–1510.

Vidal Encinas, J.M., Fernández Rodríguez, C., Prada Marcos, M.E., Fuertes Prieto, M.N., 2008. Los hombres mesolíticos de La Braña-Arintero (Valdelugueros, León): un hallazgo funerario excepcional en la vertiente meridional de la Cordillera Cantábrica. Revista de investigación, Férvedes, pp. 153–164.

Wang, Y., Yang, C., Chen, X., Zhao, N., 2006. Biomimetic formation of hydroxyapatite/collagen matrix composite. Adv. Eng. Mater. 8 (1-2), 97–100.

Watts, I., 2009. Red ochre, body painting, and language: interpreting the Blombos ochre. In: Botha, R., Knight, C. (Eds.), The Cradle of Language. Oxford University Press, Oxford, pp. 62–92.

Xie, Y., You, J., Lu, L., Wang, M., Wang, J., 2019. Raman spectroscopic study of coal samples during heating. Applied Sciences 9 (21), 4699. https://doi.org/10.3390/app9214699.